

Please cite the Published Version

Chiweshe, TT, Potgieter-Vermaak, S and Purcell, W (2019) Characterization of Chromium (III) Compounds Isolated from Different Mineral Ores Using Ammonium Phosphate as Flux. *Mining, Metallurgy and Exploration*, 36 (2). pp. 441-450. ISSN 2524-3462

DOI: <https://doi.org/10.1007/s42461-018-0010-1>

Publisher: Springer

Version: Accepted Version

Downloaded from: <https://e-space.mmu.ac.uk/623749/>

Additional Information: The final publication is available at Springer via <http://dx.doi.org/10.1007/s42461-018-0010-1>.

Enquiries:

If you have questions about this document, contact openresearch@mmu.ac.uk. Please include the URL of the record in e-space. If you believe that your, or a third party's rights have been compromised through this document please see our Take Down policy (available from <https://www.mmu.ac.uk/library/using-the-library/policies-and-guidelines>)

Characterization of chromium (III) compounds isolated from different mineral ores using ammonium phosphate as flux

Trevor T. Chiweshe¹ and Walter Purcell^{1,2*} and Sanja Potgieter-Vermaak^{3,4}

¹*Department of Chemistry, University of the Free State, Nelson Mandela Drive, Bloemfontein, 9300, South Africa*

²*School of Chemical and Metallurgical Engineering, University of the Witwatersrand, Johannesburg, South Africa*

³*Division of Chemistry & Environmental Science, Manchester Metropolitan University, Manchester, UK*

⁴*Molecular Science institute, School of Chemistry, University of the Witwatersrand, Johannesburg, South Africa*

* To whom correspondence should be addressed

E-mail: purcellw@ufs.ac.za

Abstract

Complete isolation of chromium (III) from the reference material (SARM 131), UG2 chromite ore and Merensky Reef mineral ore was achieved using ammonium phosphate salt as flux. Optimum pH (3.2 - 3.8) conditions and sample to flux ratios (1:25) were some of the factors that were critical for the complete isolation of chromium. Increasing the sample to flux ratio (1:50 excess) however resulted in the conversion of all the elements in the melt into a green solution (pH, 5.8 - 6.7). A different chromium compound was subsequently isolated from the green solution by allowing this solution to stand in an open vessel in a cupboard for a month during which time the pH decreased to pH 3.5 - 4.2. Quantitative analyses of chromium from the isolated precipitates of SARM 131, UG2 chromite ore and Merensky Reef mineral ore indicated chromium contents of 41.87, 60.41 and 23.93 % respectively which were very close to the chromium content in the original samples. Analysis of the chromium precipitates using IR indicated the presence of phosphates (1100 - 1200 cm^{-1}) whilst SEM-EDX analysis showed the presence of microscopic crystalline particles with Cr, P and O as the major elements. Further

characterization of the chromium precipitates using XRD and Raman successfully identified the product as chromium (III) metaphosphate C-type ($\text{Cr}(\text{PO}_3)_3$, JCPDS#01-077-0672) in the isolated chromium precipitates.

Key words: Ammonium phosphate, chromium metaphosphate, UG2, Merensky Reef, XRD, Raman.

Introduction

Worldwide, 85 % of chromium produced is used in the production of ferrochromium alloys (stainless steel) and chromium metal, because it is highly corrosion resistant and hard. Chromite (FeCr_2O_4) is the main chromium source and in 2015 South Africa accounted for 56% of the global chrome ore and concentrate production. Estimates indicate that the country also holds approximately 72 % of the world's chromium resources.¹ Other producers include India, Kazakhstan, Turkey and Russia.² The ferrochrome market declined slightly from 30 to 29 million tons between the year 2012 - 2014 due to the slump in the Chinese economy as well as decline in supply from South Africa due to a lack of reliable electric power supply from the state-owned power utility Eskom.³ The second quarter of 2016, however, saw increased ferrochrome demand mainly due to renewed economic growth as well as decreasing chrome stocks in China's main ports.

Commercial ferrochromium alloys are usually produced during high temperature pyrometallurgical processes (800-1400 °C), which include the silicothermic or aluminothermic processes⁴ while the chromium metal is produced by roasting and leaching, followed by reduction with carbon and aluminum. In South Africa, the biggest source of chromite (FeCr_2O_4 , 69 – 70 %,) is obtained from the Upper Group 2 deposits (UG2) in the Bushveld Igneous Complex (BIC), which is mainly beneficiated for its platinum group elements (PGE) content.⁵ The low-grade chromite concentrate, which is produced as a by-product from this process, accounts for 31 % of the country's chrome ore and concentrate production. Further development and improvements on the UG2 chromium beneficiation process may be difficult due to the ailing global/South African platinum sector, unreliable power supply, social unrest and economic constraining factors. In the PGE industry the depletion of the Merensky Reef and the subsequent switch to the UG2 ore as source of Pt and the rest of the PGE family was not without problems. The higher chromium content in the ores required furnaces to operate at higher temperatures, frequent shut-down of plants to remove the sticky chrome compounds accumulated in the furnace and the production of toxic chromium (VI) waste, which is produced as a by-product in the isolation of PGE and other metals.⁶

In previous studies we investigated both the Merensky Reef and UG2 ores from a PGE perspective.⁷ The aim of the studies was to completely dissolve these mineral samples and accurately quantify the PGE in the mineral ores. Part of the study included the selectivity and the sensitivity of PGE analysis in terms of acid type and concentration as well as the influence of easily ionized elements (EIE) on PGE recovery. The results obtained from this study unequivocally indicated that acid and EIE type, as well as acid and EIE concentrations have a profound influence on PGE recovery and that accurate matrix matching is required for proper PGE quantification.

Complete dissolution of PGE ores was initially achieved using a $\text{Na}_2\text{HPO}_4/\text{NaH}_2\text{PO}_4$ flux combination, but the high Na^+ ion content in the reaction mixture resulted in poor PGE recovery.⁷ Removal of the majority of Na^+ ions was accomplished by HCl addition, crystallization of NaCl and its removal *via* filtration. It was then decided to circumvent the EIE problem by using $(\text{NH}_4)_2\text{HPO}_4/(\text{NH}_4)\text{H}_2\text{PO}_4$ as flux salt. Complete dissolution was achieved using the ammonium salt (and NH_3 liberated during this process) and surprisingly a green, highly insoluble product precipitated from the reaction mixture. Characterization of the green insoluble product was extremely difficult, but after its successful dissolution with $(\text{NH}_4)_2\text{HPO}_4/(\text{NH}_4)\text{H}_2\text{PO}_4$ it appeared that product was a very high purity Cr compound with only trace amounts of impurities in the precipitate. The filtrate contained all the PGE and base metals with no traces Cr detected. A subsequent study on the sodium flux mixture also successfully produced a green product in a pH range between 6.5 and 6.9.⁸ However, the products isolated from the two phosphate fluxes were not the same and different in physical appearance (different green products) as well as in chemical properties.

The aim of this study was (i) to determine the factors and optimum conditions necessary for the precipitation of chromium from different mineral ores using ammonium phosphate salt as flux and (ii) to characterize and identify the products using various spectroscopic techniques such as scanning electron microscopy (SEM), energy dispersive X-ray spectroscopy (EDX), X-ray powder diffraction (XRD), infrared (IR), Raman and inductively coupled plasma optical emission spectroscopy (ICP-OES).

Chemicals, instrumentation and general experimental procedures

Reagents and labware

Diammonium hydrogen phosphate ((NH₄)₂HPO₄) (99 %), ammonium dihydrogen phosphate ((NH₄)H₂PO₄) (99 %), disodium hydrogen phosphate (Na₂HPO₄) (99 %) and sodium dihydrogen phosphate (NaH₂PO₄) (99 %) were purchased from Merck while the ceramic and the clay crucible (capacity, 80 and 100 mL respectively) were purchased from Lasec SA. The platinum crucible (capacity, 50 mL), HCl (10 M), HNO₃ (14.6 M) and the ICP multi-element standards (1 000 ppm) were purchased from Sigma-Aldrich. Ultra-pure deionised water (conductivity, 0.01 µS/cm) was used for all experimental analysis. The volumetric flasks used in this research were of Blaubrand grade (A) type and the glass beakers were of the Schott Duran type. All experimental results were reported as an average of 3 replicates correct to 2 decimal places and all weighed masses were reported accurately to 0.1 mg.

Description of the certified reference material (CRM)

The chrome ore CRM (SARM 131) used for validation purposes was purchased from Mintek and supplied by Xstrata Wonderkop Plant, South Africa. According to the certificate, the material was prepared by grinding the ore into small particle sizes of less than 75 µm using a ball mill process. The sample was then blended and packaged into 100 g units. The certified values of the elements contained in the SARM 131 are 14.60 % Al₂O₃, 41.83 % Cr₂O₃, 30.70 % Fe₂O₃, 9.15 % MgO, 0.24 % MnO, 3.13 % SiO₂, 0.94 TiO₂, 0.41 % V₂O₅ and 0.24 % CaO.

Sample description

The UG2 chromite and the Merensky Reef mineral ores were obtained from the BIC near Rustenburg. The samples were first crushed and the particle sizes were reduced to less than 75 µm using a ball mill process (Geology department, University of the Free State). The samples were dried and thoroughly homogenised to avoid segregation before use.

Instrumentation

A Barnstead Thermolyne furnace (max. temperature 1 300 °C) was used for the sample fusion procedure whilst the Eutech CyberScan (pH 1500) was used for pH measurement of the solutions. Characterization of newly isolated chromium precipitates, solid residues and products were done on a Digilab (FTS 2000) infrared (IR) spectrometer, an Oxford X-Max^N energy dispersive X-ray spectrometer (EDX) equipped with a Tescan VEGA3 scanning electron microscope (SEM) (Chemistry department, University of the Free State, Qwaqwa campus), a D8 Advance Bruker powdered X-ray diffraction spectrometer (XRD) (Physics department, University of the Free State) and a Renishaw InVia Raman spectrometer (Division of Chemistry and Environmental sciences, Manchester Metropolitan University, UK). A Shimadzu ICPS-7510 ICP-OES with a radial sequential plasma spectrometer was used for elemental analysis. Default settings/conditions were used for the ICP-OES as shown in Table 1 in order to achieve the best precision and accuracy of results.

Experimental procedures

Calibration standards

ICP-OES multi-element calibration standards

Multi-element calibration standard solutions were prepared from the original standard solutions (1 000 ppm) and diluted to concentrations between 0.5 and 10.0 ppm in 100.0 mL volumetric flasks using a ‘Transferpette’ micro-pipette. Hydrochloric acid (5.0 mL; 10 M) was added and the flasks were filled to the mark using ultra-pure deionised water (conductivity, 0.01 μ S/cm).

Sample preparation and isolation of chromium from the SARM 131 reference material, UG2 and Merensky Reef samples

The SARM 131,UG2 chromite and Merensky Reef mineral ores were first homogenized with shakers for 48 hours and then dried at 110 °C in an oven for 24 hours. Samples (0.5 g) of each ore was thoroughly mixed with excess amounts of salt (flux)

$(\text{NH}_4)_2\text{HPO}_4/(\text{NH}_4)\text{H}_2\text{PO}_4$ in the ratio of 1:25. The resultant mixtures were all quantitatively transferred into separate platinum crucibles (ceramic and clay crucibles were also used, but proved to be ineffective – see discussion in the first paragraph) and heated in a furnace at 800 °C until molten liquids were obtained (\pm 20 min). The molten green melts were cooled at room temperature and the glassy-green melts were dissolved in deionized water to yield mixtures containing green precipitates and light yellowish solutions. The resultant mixtures were heated in HCl (10 mL; 10 M) until a green “chartreuse” mixture was formed. The mixtures were cooled and filtered at room temperature and the collected green precipitate and the yellow filtrate were analysed separately.

Quantitative analysis of the yellow filtrates and green precipitates obtained after fusion of SARM 131, Merensky Reef and UG2 chromite samples

Filtrate:

The yellow filtrates of SARM 131, UG2 chromite and Merensky Reef samples were quantitatively transferred into separate volumetric flasks and HCl acid (2.0 mL; 10 M) was added. The flasks were filled to the mark using deionised water before being homogenised and quantitatively analysed for the metal content using ICP-OES.

Solid characterisation:

The dried powdered green samples (*ca.* 0.5 g) obtained from SARM 131, UG2 chromite and Merensky Reef ores were subsequently characterized with SEM-EDX, XRD (analysed externally), IR and Raman spectroscopy. Samples analysed using Raman spectroscopy were mounted on double-sided carbon tape fixed onto glass microscope slides. The mounting of the sample involved putting a small amount on the tape and then removing excess by tapping it on the side of the microscope slide. In this way, particles were sparsely fixed to the adhesive surface to facilitate single particle analysis. Samples were analysed using either a Renishaw InVia Raman microscope or a DXR Raman scope fitted with a Peltier-cooled charge-coupled device detector. The source of excitement was a 514.5 nm Ar^+ laser in the case of the Renishaw and 532 or 780 nm in the case of the latter instrument.

The instrument was calibrated at the beginning of each set of analysis using a silicon chip; each time a peak was achieved at $520.5 \text{ cm}^{-1} \pm 0.05 \text{ cm}^{-1}$ with an intensity that was monitored over time. In general, the instrument was used in extended mode, limiting the spectral range from 100 to 2200 wavenumbers and the number of acquisitions varied between 1 and 410-second exposures to ensure an acceptable S/N ratio. The power density varied between 2 – 8 mW at the sample. Data acquisition was carried out with the Wire™ and Spectracalc software packages from Renishaw. Spectral identification was done using an in-house spectral library for the iron oxides, the RRUFF database and a commercially available spectral library via Spectracalc software (GRAMS, Galactic Industries).

Wet characterization:

For the wet chemical analysis, green precipitates were digested using sodium phosphate or excess ammonium phosphate salt (1:50). In the event of using sodium phosphate salt, EIE were removed as white crystals (Na^+ ions as confirmed by ICP-OES analysis) by adding HCl (20 mL; 10 M) to the resultant green solutions and left to stand overnight. The resultant green melts were dissolved in deionised water and transferred into separate volumetric flasks. Hydrochloric acid (2.0 mL; 10 M) was added to each flask and filled to the mark using deionised water. The resultant green solutions were quantitatively analysed for the metal content using ICP-OES.

Determination of the sample: flux ratios using the SARM 131 reference material

Samples (0.5 g) of the previously dried SARM 131 reference material were accurately (0.1 mg) weighed and mixed with the ammonium salt (flux) in the ratios of (i) 1:12.5 and (ii) 1:50 (excess) respectively. The samples were transferred to platinum crucibles and digested for ± 20 min at $800 \text{ }^\circ\text{C}$ until molten liquids were formed. A mixture of the green melt and greyish particles settled at the bottom of the crucible indicating the incomplete dissolution of SARM 131 with 1:12.5 mineral to flux ratio. Complete sample dissolution was achieved with the 1:50 sample to flux ratio and the resultant green melt from (ii) was dissolved in deionised water (100 mL) and a transparent green solution was formed.

Determination of the influence of pH in the precipitation of chromium using the SARM 131 reference material

The effect of pH was determined using the same experimental conditions as the determination of the sample: flux ratio. The resultant solutions or mixtures of the SARM 131 samples obtained after fusion using sample flux ratio (i) 1:25 and (ii) 1:50 were measured using a calibrated pH meter (calibrated using a buffer solution at pH 4, 7 and 10). Resultant mixtures from (i) (where chromium was instantly precipitated) had a pH in the range of 3.2 - 3.8 whilst solutions from (ii) (where no chromium was precipitated, transparent green solution) had pH in the range of 5.8 - 6.7. Precipitation of an emerald green substance (~50 mg) from this transparent green solution happened by chance and was isolated after the green solution was left to stand (~30 days) in a cupboard during which the pH decreased to 3.8. The emerald green precipitate was dried and analysed using IR, XRD and Raman spectroscopy.

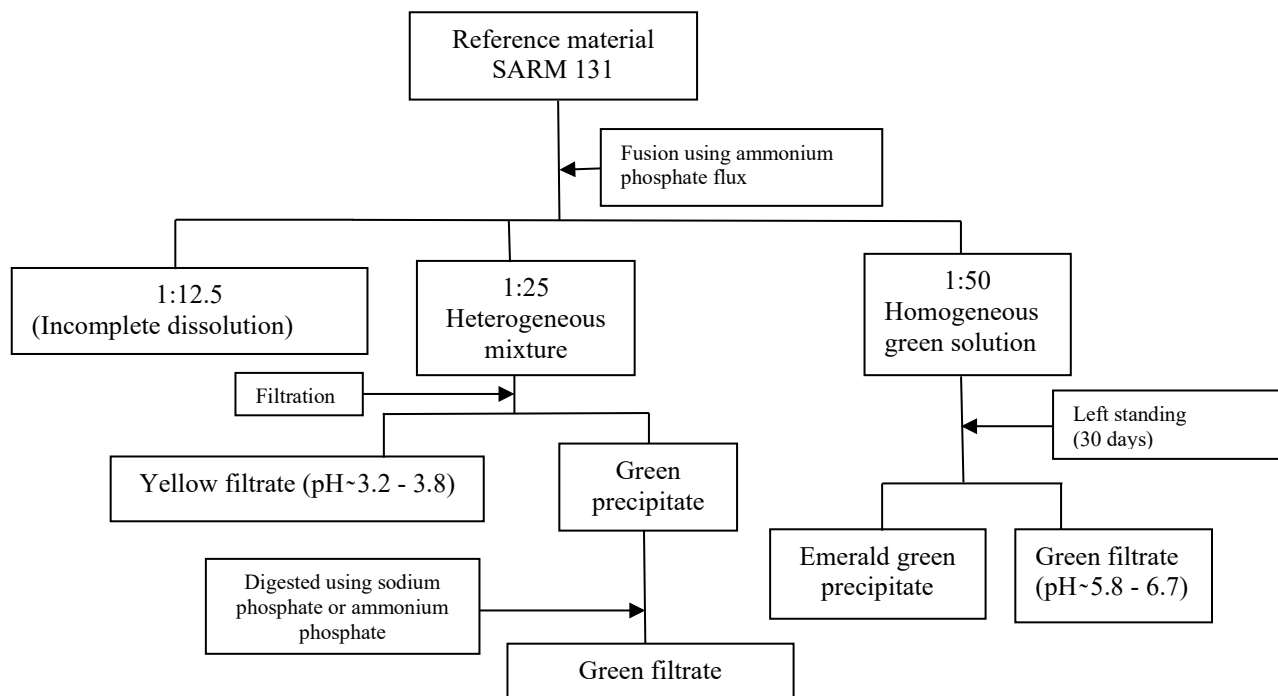
Results and discussion

Fusion of SARM 131, Merensky Reef and UG2 samples using ammonium phosphate salts $(\text{NH}_4)_2\text{HPO}_4/(\text{NH}_4)\text{H}_2\text{PO}_4$

Fusion of the SARM 131 reference material was first attempted using ceramic (m.p. 1 300 °C) and clay (m.p. 1 200 °C) crucibles and results obtained showed that both the crucibles were not compatible for fusion using ammonium phosphate flux. All sample preparation procedures were therefore conducted using platinum crucible (m.p. 1 768 °C). The resultant green glassy melt from the SARM 131 were subsequently solubilized using deionised water to yield mixtures of green precipitate and light yellow filtrate solutions (Scheme 1). Complete dissolution of SARM 131, Merensky Reef and the UG2 chromite ores required that both the flux (ammonium phosphate salt) and the sample's particle size be closely matched (75 µm). Unmatched particle sizes between the sample and the flux were found to segregate and resulted in the incomplete dissolution of the mineral sample. Qualitative analysis of the green precipitate showed the presence of Cr (> 1 000 ppm) and traces amounts of Al, Cu and Fe (< 1 ppm). Qualitative analysis of the light yellow filtrate solution showed the presence of twenty elements, which included Al, Ca, Fe and Mg

(above 10 ppm) and In, Mn, Ni, Os, Pb, Pt, Ru, Si, Sr, Ba, Cu, Co, Ga, Ti, V and Zn (below 10 ppm).

The variation of sample: flux ratio was the first step in the investigation to determine the possible factors that determine chromium precipitation formation. The initial experimental conditions indicated that chromium precipitation formation from the glassy melt occurred at a sample: flux ratio of 1:25. Decreasing the ratio to 1:12.5 resulted in the incomplete fusion (digestion) of the SARM 131 sample (Scheme 1), which was evidenced by the presence of light brown powdered particles of the starting material. Increasing the flux ratio to 1:50 again resulted in the formation of the green glassy melt, which dissolved easily in deionised water to yield a clear green solution and interestingly, no precipitation formation. The precipitation of chromium in the 1:25 sample to flux ratio was assumed to be the result or connected to the production of NH_3 gas during the fusion process and attributed to a possible pH changes in the melt. Variation in the flux ratios (Scheme 1) was also considered to influence the precipitation of chromium due to formation of different types of metal complexes as a result of the variation of the phosphate concentration and/or pH changes.⁹



Scheme 1: Flow chart of the analysis of the sample: flux ratio in the dissolution of SARM 131 using ammonium phosphate salt as flux

The influence of pH was performed by varying the sample: flux ratios to determine whether these changes had any effect on chromium precipitation. The SARM 131 sample digested at a 1:25 ratio, which resulted in the instant precipitation of chromium had a pH between 3.2 and 3.8, whilst the sample digested 1:50 sample to flux ratio yielded no chromium precipitate and the solution had a pH between 5.8 and 6.7. Other noticeable difference between the two melts was the easy dissolution of the 1:50 product (compared to the highly insoluble 1:25 green precipitate) into a clear green solution (with the addition of water), which may be attributed to a different kind of product formed at the higher flux ratios. Further analysis on the green solution obtained after digesting the SARM 131 using excess flux 1:50 revealed a gradual precipitation of an emerald green residue after the green solution was isolated after a month. Qualitative analysis of the emerald green residue revealed very similar results as previously obtained from the first precipitate (1:25 ratio) showing the presence of large amounts of Cr (> 1 000 ppm) and trace amounts of Al, Cu and Fe (< 1 ppm).

Quantitative analysis of chromium and other elements in the SARM 131 reference material, UG2 chromite and Merensky Reef mineral ores using ICP-OES

Elemental analysis of the SARM 131 reference sample, UG2 chromite ore as well as the Merensky Reef ore was performed using ICP-OES analysis (Table 2). The reference SARM 131 sample was first analysed to establish measurement traceability (comparison with certified values). These results indicated an excellent correlation between the experimental and certified values, especially for Cr₂O₃ with recovery of 41.87 % compared to the certified value of 41.83 %. The percentage Cr₂O₃ content was the highest in the sample, followed by Fe₂O₃ (32.35 %), Al₂O₃ (14.34 %), MgO (9.22 %) and SiO₂ (4.30 %). The presence of Cr, Fe, Mg and Al as major elements in SARM 131 corresponds to the general chromite formula, (Mg²⁺, Fe²⁺)O(Cr³⁺, Al³⁺, Fe³⁺)₂O₄, which suggests that the reference material was of a chromite origin. These results not only confirm the success of the dissolution method, but also measurement traceability and method validity.

As expected, substantial amounts of chromium (Cr_2O_3) were present in the UG2 chromite ore (60.41 %) while lower chromium content were obtained for the Merensky Reef (23.93 %). Other major elements obtained in the UG2 chromite ore sample included Fe_2O_3 (25.69 %), MgO (8.06 %) and SiO_2 (5.50 %). Major elements found in the Merensky Reef included Al_2O_3 (10.83 %), CaO (4.83 %), Fe_2O_3 (23.93 %), MgO (8.77 %) and SiO_2 (10.53 %). Analysis of the Fe:Cr ratio in SARM 131, Merensky Reef and UG2 ore were 1:1.3, 1:1.4 and 1:2.3, respectively. The higher Fe:Cr ratio in the UG2 chromite compared to the Merensky Reef ore confirms the abundance of chromium in the UG2 layer, which is currently exploited for PGE and ferrochrome production.¹⁰ The higher chromium content in the UG2 chromite ore (60.41 %) compared to the Merensky Reef (23.93 %) also illustrates the current challenges and difficulties faced in the metallurgical extraction of precious metals in the UG2 Reef.¹¹

Characterization of the chromium precipitates isolated from the SARM 131 reference sample, Merensky Reef and UG2 mineral ore using IR, SEM-EDX, XRD and Raman spectroscopy.

IR characterization

The chromium precipitates obtained after the flux fusion step for the three different samples were initially characterized using IR spectroscopy. The IR spectra of the chromium precipitates, including the emerald green precipitates, were compared with that of the ammonium phosphate (starting material) to determine any changes in the stretching frequencies. A comparison of the chromium precipitate spectra of SARM 131, Merensky Reef, UG2 chromite and emerald green precipitates revealed similarities in the stretching frequencies of these products. Further comparison of the chromium precipitate spectra with ammonium phosphate (starting material) showed peak differences in the region of 980 cm^{-1} and below 700 cm^{-1} (Figure 1), which were not present in the starting material. All the IR spectra for the chromium precipitates and the emerald green precipitate showed the presence of one common peak in the region of $1\ 200\text{ cm}^{-1}$, which indicates the presence of phosphates ($1\ 100 - 1\ 200\text{ cm}^{-1}$).¹² The similarity in the IR spectra for all the chromium

precipitates and the emerald green precipitate revealed the possibility of the same chromium product.

SEM-EDX characterization

SEM-EDX analyses were also performed on the four products, which included the SARM 131, UG2, Merensky and the emerald green precipitate. The SEM results of the isolated chromium precipitates (Figure 2) for both the UG2 and the SARM 131 showed a micro-crystalline, cubic crystal-like structure, which suggested the possibility of a pure and a similar chromium product. The Merensky product was visually different with larger and more irregular, almost amorphous-like particles.

The EDX spectra showed an increase in emission intensities from Cr<O<P (Table 3) while the qualitative results reported the presence of Al, Cr, P, O and Si as major elements in all the isolated products, with smaller amounts of Fe, Al, Si and Cu in all the samples. The Cr:O:P intensity peaks obtained for all the samples confirmed the presence of phosphate like ligands in the final products. The large amount of iron present in UG2 sample was unexpected since the dissolution of this green precipate indicated trace amounts of iron with the ICP analysis. The Cr: P: O ratio of 1: 3: 4 points to a phosphate polymer or a phosphate compound (CrP_3O_4).¹³

The summary of the chemical composition of the green precipitates in Table 3 indicated lower than the expected phosphorous content for all the precipitates compared to $\text{Cr}(\text{PO}_3)_3$ found with XRD. Lower than expected oxygen was observed for the SARM 131 sample. In all the samples the Cr content was also lower than the theoretical/expected value, but interestingly the combined metal content (Cr plus Fe) for the UG2 and SARM 131 were almost equal to the expected percentage chromium content. This can be attributed to the possible inclusion of Fe atoms into the Cr phosphate structure or the presence of some Fe phosphate crystals with the isolated Cr phosphate precipitate. This discrepancy needs to be investigated and clarified.

XRD characterization

The chromium precipitates were characterized further using powder XRD to identify exact chemical compositions. The XRD patterns obtained for the chromium precipitates, SARM 131 (1:25 and 1:50 ratios), UG2 chromite, Merensky Reef ore and emerald green precipitate as well as the $\text{Cr}(\text{PO}_3)_3$ crystal structure¹⁴ were compared against the different reported XRD patterns in the The International Centre for Diffraction Data base or the Joint Committee on Powder Diffraction Standards data base¹⁵ (Figure 3).

The XRD patterns of the three chromium precipitates, SARM 131 (1:25 ratio), UG2 chromite, Merensky Reef ore as well as the $\text{Cr}(\text{PO}_3)_3$ (JZ1135) showed similar 2θ patterns to that of $\text{Cr}(\text{PO}_3)_3$ (JCPDS#01-077-0672, Joint Committee on Powder Diffraction Standards), which is catalogued as $\text{Cr}(\text{PO}_3)_3$ with the strongest peak intensities in the region of 22.81 and 26.01 (2θ) degrees. This suggested the presence of similar products in the isolated compounds, which compared favourably with $\text{Cr}(\text{PO}_3)_3$. The small anomalies in the XRD patterns of all these chromium precipitates may be the result of the formation of other metaphosphates from impurities (Al, In, Ti, V, Fe and Ru)¹⁴, which might have co-precipitated with chromium. The XRD peak intensities in the region of 26.01 degrees (2θ) increased from SARM 131 < UG2 chromite < Merensky Reef < emerald green precipitate, which suggested a shift in the morphological structure of the precipitates, from the highly crystalline (SARM 131 and UG2) products to the more amorphous Merensky and emerald green precipitates. This increase in the relative intensity at 26 ° is attributed to the increasing dominance of the 3.5,-2 (h,k,l) reflection for the more crystalline products compared to the more amorphous type compounds.

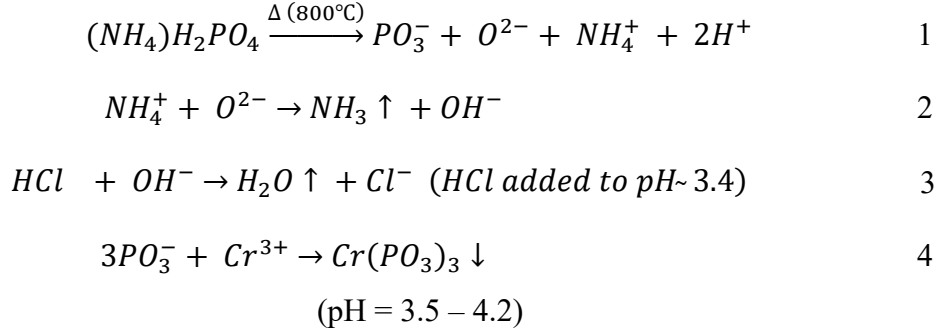
However, closer inspection of the peak positions (Table 4) and the relative intensities of the XRD patterns of each chromium precipitate (e.g., peak height) pointed to different morphological structures. The results in Table 4 clearly illustrate the difference in the actual 2θ positions of the different precipitates. The powder peak positions, as well as the relative intensities, especially at 26.10 ° (Figure 3) and the poor crystalline product (Figure 2) of the Merensky ore correlates very well with the cited values and intensities reported for JCPDS # 01-077-0672 ($\text{Cr}(\text{PO}_3)_3$). On the other hand, the powder peak positions and peak intensities, especially at 26.27 °, for both the UG2 and the SARM 131 samples with the more crystalline product (Figure 2), as well as higher Cr content in original samples

(Table 2) are much more in line with that obtained for the isolated and structurally characterized $\text{Cr}(\text{PO}_3)_3$ polymer that was reported by Yakubovich¹⁵ and Gruss.^{14,16} It would therefore appear that the XRD powder patterns of the Gruss product and that of the isolated UG2 and SARM 131 is a more and better presentation of $\text{Cr}(\text{PO}_3)_3$ than the current XRD spectrum in the JCPDS (more crystalline and the peak intensity at 26.27° (h,k,l: 3,5,-2). The XRD pattern of the emerald green precipitate, isolated after 30 days, may contain some $\text{Cr}(\text{PO}_3)_3$ and possibly different mixtures of other products, which might have resulted in the amorphous structure revealed in the SEM images (Figure 2).

Except for the emerald green precipitate, the XRD analysis clearly identified the products isolated from the $(\text{NH}_4)_2\text{HPO}_4/(\text{NH}_4)\text{H}_2\text{PO}_4$ flux fusion as the chromium metaphosphate compound $\text{Cr}(\text{PO}_3)_3$, (JCPDS#01-077-0672). Six different chromium metaphosphates are reported in literature (i.e. A, B, C, D, E and F-types), but only two (i.e., B and C) have been identified and isolated. The products isolated from the phosphate flux fusion is of the monoclinic C-type (Figure 4).^{17,18,19}

The formation of $\text{Cr}(\text{PO}_3)_3$ from the fusion of the reference material (SARM 131), UG2 chromite, and Merensky Reef ore using ammonium phosphate was very unusual and unexpected. Often, $\text{Cr}(\text{PO}_3)_3$ metaphosphates are synthesised from mixing chromium (III) nitrate with the dibasic $(\text{NH}_4)_2\text{HPO}_4$ (m.p. 155°C) (ratio 1:3) in acidic medium (HNO_3) and the mixture is then heated in air at 800°C for 7 days, which results in the formation of micro-crystalline C-type $\text{Cr}(\text{PO}_3)_3$.¹¹ The formation of C-type $\text{Cr}(\text{PO}_3)_3$ in this research presents an alternative or new method of separating the chromium in geological mineral ores as metaphosphates using $(\text{NH}_4)_2\text{HPO}_4$ at 800°C for few minutes (± 20 min).

A possible mechanism for the formation of the C-type $\text{Cr}(\text{PO}_3)_3$ from the chromium mineral ores obtained in this study can be presented in the following reactions:



It is a well-known fact that phosphates decompose (Equation 1) at temperatures above 151 °C to form the metaphosphates.²⁰ The production or liberation of NH₃ gas was evident from the fumes liberated during the flux dissolution/decomposition reaction and may be attributed to the reaction of a strong base (O²⁻) with the ammonium ions according to Equation 2. Finally the Cr ions in the liquid solution react with the metaphosphate ions to produce the isolated product (Equation 3).

Raman characterization

The white light images of the SARM 131, Merensky and UG2 samples revealed particles that varied in colour from white-grey to black. Crystalline particles were angular in appearance and cuboid in shape. Particles displayed similar spectra (Figure 5), often superimposed on the amorphous carbon spectrum. The black inclusions presented the typical amorphous carbon spectrum with a clear graphitic (G-band) at around 1 600 cm⁻¹ and a disordered (D-band) at around 1 350 cm⁻¹. Some of the particles were laser sensitive and fluoresced, but these were limited. The most prominent peak was displayed at 1 226 cm⁻¹, which sometimes had a shoulder at around 1 185 cm⁻¹, which could be assigned to the asymmetric and symmetric vibrations of the PO₂ group of the metaphosphate, respectively²¹. Strong peaks were observed at 672, 428, and sometimes 413 cm⁻¹ (potentially due to vibrations of POP) and medium intensity bands at 512, 332, 370, 287 cm⁻¹. It seems therefore, that the Raman spectra in general confirm the formation of chromium metaphosphate.

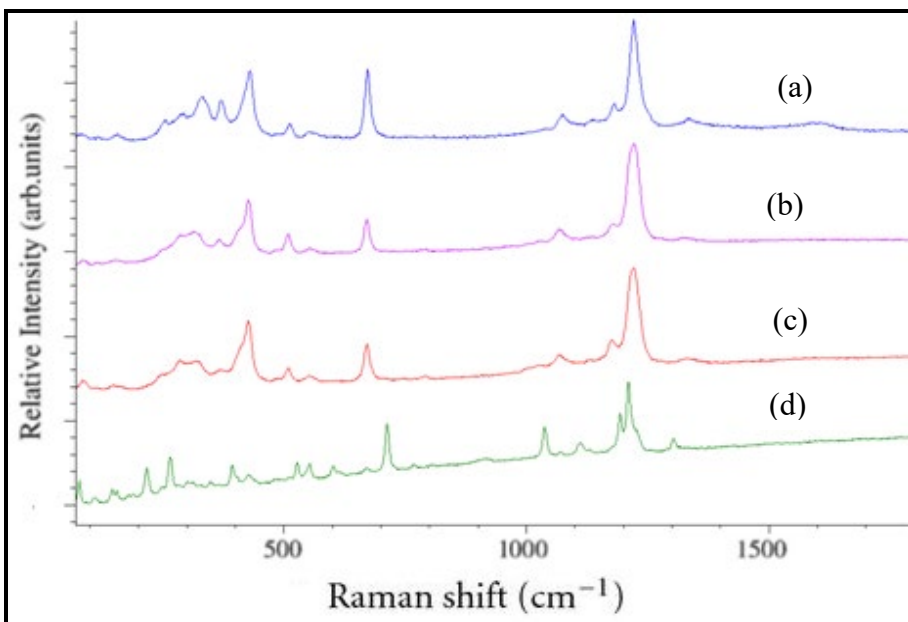


Figure 5: Raman spectroscopy of the (a) SARM 131, (b) UG2 chromite (c) Merensky Reef, and (d) the emerald green precipitate

The white light images of the emerald green precipitate revealed particles that varied in colour from bright white-grey to vivid emerald green. Some dark inclusions were observed, but did not display a good spectrum. Crystalline particles were angular in appearance and cuboid in shape and the particles displayed similar spectra, but could not be analysed using the green visible wavelength laser due to fluorescence. The 780 nm laser produced spectra that were similar to that of Merensky showing the most prominent peak at $1\,226\text{ cm}^{-1}$, followed by strong peaks at 672 and 428 cm^{-1} and medium intensity bands at 512 , 332 , 370 and 287 cm^{-1} .

Conclusion

Complete digestion and the subsequent isolation of chromium from the reference material (SARM 131), UG2 chromite and Merensky Reef mineral ore was achieved using ammonium phosphate salt as flux. Qualitative analysis of the chromium precipitate shows the presence of Cr with trace amounts of Mg, Ca and Na. Analysis using IR and Raman spectroscopy revealed the presence of phosphates whilst SEM-EDX analysis showed

micro-crystalline images of the chromium precipitate and the presence of Cr, P and O as major elements. The XRD analysis confirmed the presence of $\text{Cr}(\text{PO}_3)_3$ for all the resultant chromium precipitates. It was therefore concluded that fusion of the geological samples containing chromium using ammonium phosphate salt, precipitates all the chromium as $\text{Cr}(\text{PO}_3)_3$, which can be beneficial in the hydrometallurgical processing of precious metals.

Acknowledgements

The authors thank the Research Fund of the University of the Free State and the National Research fund of South Africa for the financial support.

References

1. <http://www.miningweekly.com/print-version/south-africas-chrome-industry-well-placed-to-grow-and-prosper-2016-10-21>
2. L. Racon, 2014 a record year for ferrochrome only - Minerals & Metals Review, 2015, June: 48 - 49.
3. <http://www.polity.org.za/article/strong-outlook-for-recovering-ferrochrome-industry-merafe-2017-03-08>
4. R.T. Jones and T.R. Curr, Southern African Pyrometallurgy, 2006, 127 - 150.
5. L.W. Schurmann, P.J. Grabe, C.J. Steenkamp, *Chromium In The Mineral Resources of South Africa*; Council for Geoscience Handbook, (6th Ed), 1998, 16, 90 - 105.
6. A.R. Barnes and A.F. Newall, Spinel Removal from PGM Smelting Furnaces, Southern African Pyrometallurgy, 2006, 77 - 88.
7. T.T. Chiweshe, W. Purcell and J.A. Venter, *Journal of the Minerals, Metals and Materials Society (JOM)*, 2016, 68 (6), 1691 - 1700.
8. T.T. Chiweshe and W. Purcell, *Chromium isolation from different mineral ores*, Conference proceeding of EMC, 2017, 1 - 15.
9. J.M. Rojo, J.L. Mesa, L. Lezama and T. Rojo, *J. Mater. Chem.*, 1997, 7(11), 2243.
10. L.W. Schurmann, P.J. Grabe, C.J. Steenkamp, *Chromium In The Mineral Resources of South Africa*; Council for Geoscience Handbook, (6th Ed), 1998, 16, 90 - 105.

-
11. J.A. Kinnaird, F.J. Kruger, P.A.M. Nex, R.G. Cawthorn, *Applied Earth Science, Transactions of the Institutions of Mining and Metallurgy: Section B*, 2002, 111(1).
12. B. Stuart, *Infrared Spectroscopy: Fundamentals and Applications* John Wiley & Sons, Ltd., 2004, 84.
13. H. Fuks, S.M Kaczmarek, M. Bosacka, *Review of Advanced Material Science.*, 2010, 23, 57 - 63.
- 14.M. Gruss and R. Glaum, *Acta Crystallogr., Sect. C*, 1996, 52, 2647.
15. O.V. Yakubovich, O.V. Dimitrova, G.V. Savina, *Kristallografiya*, 1991, 36, 486.
16. <http://scripts.iucr.org/cgi-bin/sendcif?jz1135sup1-2017-05-08>
- 17.L.K. Elbouaanani, B. Malaman and R. Gerardin, *J. Solid State Chem.*, 1999, 148, 455.
- 18.M. Bagieu-Boucher and J.C. Guitel, *Acta Crystallogr., Sect. B*, 1977, 33, 2529.
19. P. Remy and A. Boule, *Bull. Soc. Chim. Fr.*, 1972, 2213 - 2221.
20. M. Banach and A. Makara, *J. Chem. Eng. Data*, 2011, 56, 3095 - 3099.

21 P. Godlewska, A. Matraszek, S.M. Kaczmanek, H. Fuks, T. Skibinski, K. Hermanowicz, M. Ptak, I. Szczygiel, L. Macalik, R.Lisiecki, W. Ryba-Romanowski and J. Hanuza, *J. Lumin*, 2014, 146, 342 - 350.

List of Figures

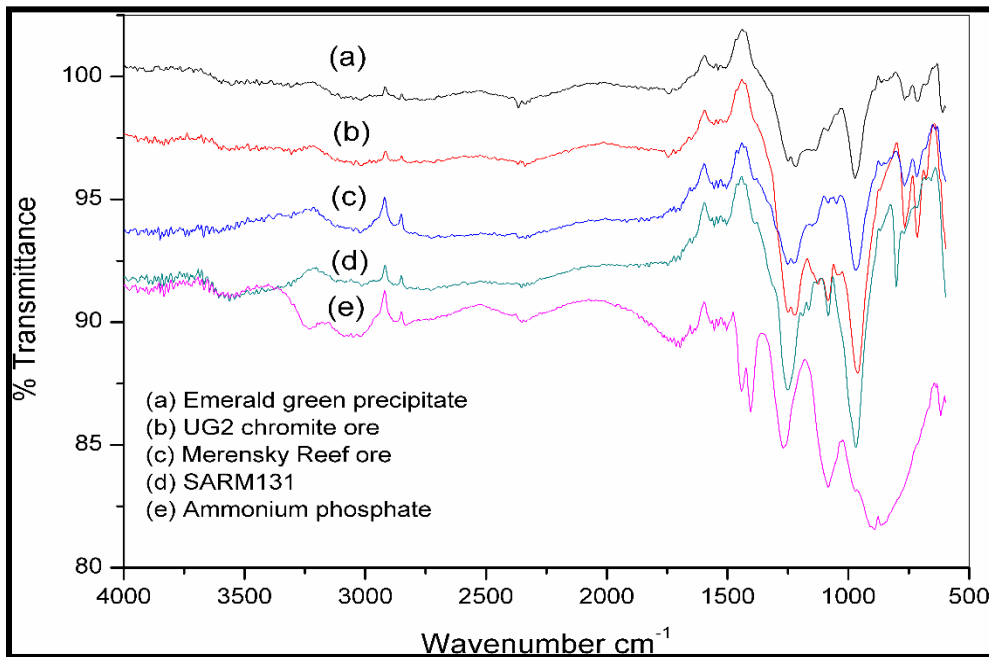


Figure 1: Infrared red (IR) spectrums of the green chromium precipitates obtained from the SARM 131 and the emerald green precipitate, UG2 chromite ore and Merensky Reef ore compared with the spectrum of ammonium phosphate flux.

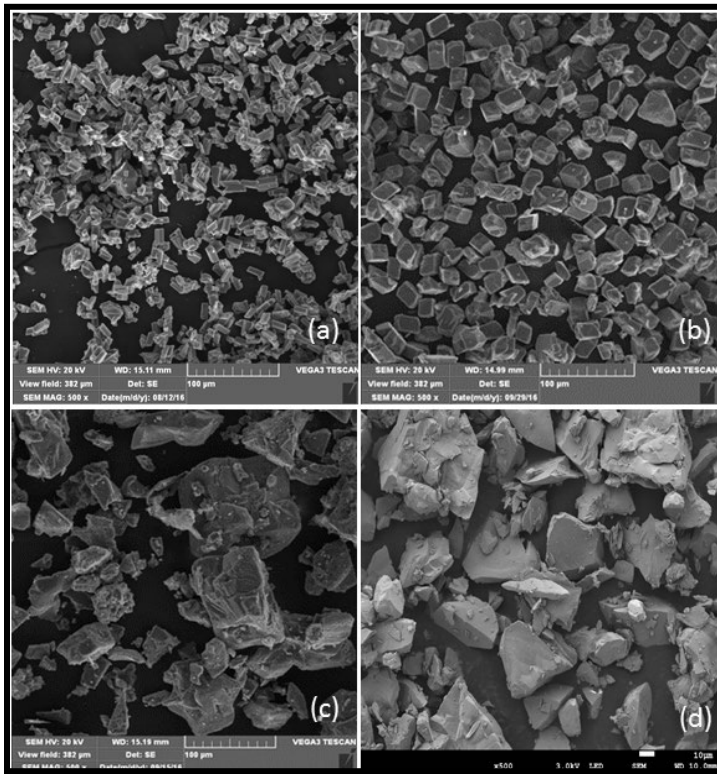


Figure 2: SEM images of the chromium precipitate obtained from (a) SARM 131, (b) UG2 chromite ore (c) Merensky Reef ore and (d) emerald green precipitate

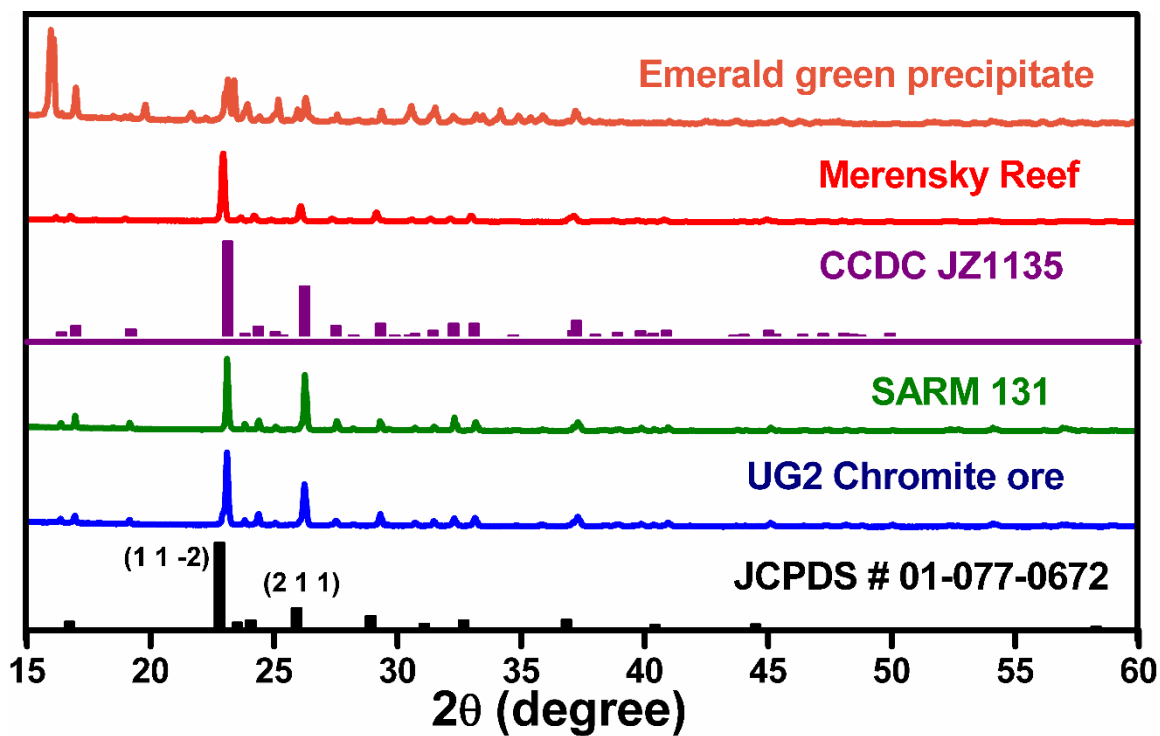


Figure 3: The XRD patterns of the Merensky Reef, SARM 131, UG2 chromite ores and the emerald green precipitate compared with the reference pattern of the C-type Cr(PO₃)₃ (JCPDS # 01-077-0672) and the Cr(PO₃)₃ crystal structure (JZ1135)

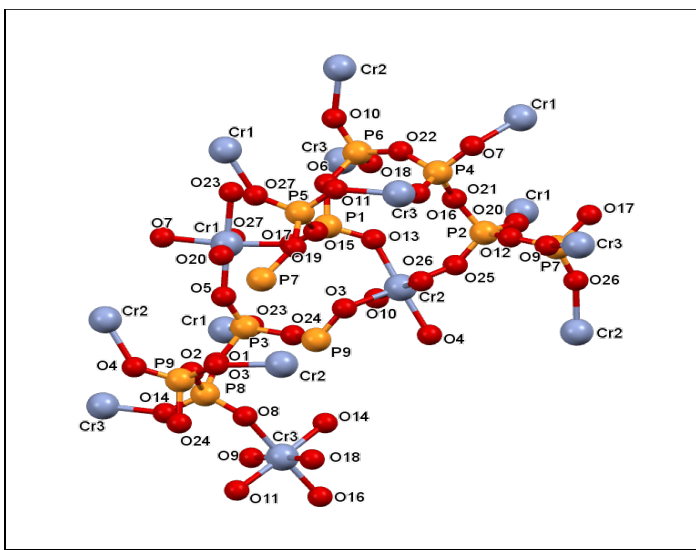


Figure 4: Crystal structure of C-type $\text{Cr}(\text{PO}_3)_3$ ¹⁴

List of Tables

Table 1: Selected optimum ICP-OES operating conditions for metal analysis

| Parameter | Condition |
|------------------------|------------------|
| RF power | 1.2 kW |
| Coolant gas flow rate | 14.0 L/min |
| Plasma gas flow rate | 1.2 L/min |
| Carrier gas flow rate | 0.7 L/min |
| Sample uptake method | Peristaltic pump |
| Type of spray chamber | Glass cyclonic |
| Type of nebulizer | Concentric |
| Injector tube diameter | 3.0 |

Table 2: ICP-OES quantitative analysis of the metal oxide content in the green precipitate and yellow filtrates of SARM 131, Merensky Reef and UG2 chromite samples after fusion with $\text{NH}_4\text{H}_2\text{PO}_4/(\text{NH}_4)_2\text{HPO}_4 \cdot \text{H}_2\text{O}$ flux

| <i>Elements</i> | SARM 131 % | UG2 chromite % | | Merensky Reef % | | | |
|---|-------------------------|-----------------|--------------------|-----------------|--------------------|----------|-----------------|
| | <i>Certified values</i> | <i>Filtrate</i> | <i>Precipitate</i> | <i>Filtrate</i> | <i>Precipitate</i> | | |
| Al_2O_3 | 14.60 | 15.87 (3) | 0.007(2) | 0.09(2) | 0.02 (1) | 10.83(1) | 0.03(2) |
| BaO | - | 0.04(1) | | 0.02(1) | | 0.02(1) | |
| CaO | 0.24 | 2.80(6) | | 0.88(1) | | 4.83(8) | |
| CuO | - | 0.14(1) | 0.01(1) | 0.04(1) | 0.01(2) | 0.01(1) | 0.09(4) |
| CoO | - | 0.06(1) | | 0.13(1) | | 0.03(1) | |
| Cr_2O_3 | 41.83 | - | 41.87(1) | - | 60.41(4) | - | 23.93(3) |
| Fe_2O_3 | 30.70 | 30.35(6) | 0.003(1) | 25.69(1) | 0.034(2) | 18.39(4) | 0.044(3) |
| Ga_2O_3 | - | 0.06(1) | | 0.05(1) | | 0.03(1) | |
| In_2O_3 | - | 0.36(1) | | 0.19(1) | | 0.12(1) | |
| MgO | 9.15 | 9.22(2) | | 8.06(6) | | 8.77(1) | |
| MnO | 0.24 | 0.43(4) | | 0.30(1) | | 0.24(1) | |
| NiO | - | 0.31(4) | | 0.24(1) | | 0.17(1) | |
| Os | - | 0.49(7) | | 0.46(2) | | 0.33(1) | |
| PbO | - | 0.05(6) | | 0.05(1) | | 0.03(1) | |
| Pt | - | 0.19(3) | | 0.91(1) | | 0.14(1) | |
| Ru | - | 0.41(1) | | 0.25(1) | | 0.30(1) | |
| SiO_2 | 3.13 | 4.30(2) | | 5.50(1) | | 10.53(3) | |

| | | | | |
|-------------------------------|------|---------|---------|---------|
| SrO | - | 0.01(1) | 0.01(1) | 0.01(1) |
| TiO ₂ | 0.94 | 0.92(1) | 0.62(1) | 0.67(2) |
| V ₂ O ₅ | 0.41 | 0.64(2) | 0.58(1) | 0.09(1) |
| ZnO | - | 0.14(1) | 0.11(1) | 0.09(1) |

-No certified values provided/Element not present

-Bolded element(s) relates to the theme of the article

Table 3: Quantitative results obtained from the EDX analyses of the different isolated products

| Compound | Elemental (%) | | | |
|---|---------------|-------|------|-----|
| | Cr | P | O | Fe |
| Cr(PO₃)₃ ^[14] | 18.0 | 32.2 | 49.8 | - |
| Merensky | 12.1 | 31.5 | 49.5 | 2.1 |
| SARM 131 | 13.0 | 33.2 | 44.8 | 4.4 |
| UG2 chromite | 13.6 | 32.8 | 47.7 | 3.6 |
| Emerald Green | 11.52 | 32.03 | 46.0 | 4.6 |

Table 4: XRD characterization (2θ data) of the different isolated products

| Compound | 2θ/° (h,k,l) | | | | | |
|---|---------------|----------------|----------------|----------------|---------------|----------------|
| | 16.66 (1,1,0) | 22.83 (1,1,-2) | 26.02 (2,1,1) | 29.01 (0,1,3) | 32.86 (3,1,0) | 37.04 (2,2,-2) |
| Ref* | 16.66 (1,1,0) | 22.83 (1,1,-2) | 26.02 (2,1,1) | 29.01 (0,1,3) | 32.86 (3,1,0) | 37.04 (2,2,-2) |
| Merensky | 16.66 | 22.85 | 26.10 | 29.16 | 32.85 | 37.12 |
| SARM 131 | 16.92 | 23.13 | 26.27 | 29.33 | 33.13 | 37.29 |
| UG2 chromite | 16.92 | 23.13 | 26.27 | 29.33 | 33.13 | 37.29 |
| Emerald | 16.92 | 23.22 | 26.27 | 29.33 | 33.40 | 37.20 |
| Cr(PO₃)₃ ^[14] | 16.98 (2,0,0) | 23.12 (1,3,1) | 26.24 (3,5,-2) | 29.32 (3,1,-3) | 33.11 (1,3,2) | 37.28 (3,3,1) |

Ref* = JCPDS # 01-077-0672